

RELATIVISTIC SEPARABLE INTERACTION KERNEL OF THE NEUTRON-PROTON SYSTEM WITH INELASTICITIES

S.G. Bondarenko^{1†}, V.V. Burov¹, E.P. Rogochaya²

(1) *Bogoliubov Laboratory of Theoretical Physics,
Joint Institute for Nuclear Research, Dubna, Russia*

(2) *Veksler and Baldin Laboratory of High Energy Physics,
Joint Institute for Nuclear Research, Dubna, Russia*

† *E-mail: bondarenko@jinr.ru*

Abstract

Within a covariant Bethe-Salpeter approach, the relativistic complex separable neutron-proton interaction kernel is proposed. The uncoupled partial-wave states with the total angular momentum $J=0,1$ are considered. The multirank separable potentials elaborated earlier are real-valued and, therefore, enable to describe the elastic part (phase shifts, low-energy parameters, etc.) of the scattering only. The description of the inelasticity parameter comes out of the imaginary part introduced into them. To obtain parameters of the complex potentials the elastic neutron-proton scattering experimental data up to 3 GeV are used. A signal of dybaryon resonances in the ${}^3P_0^+$ partial-wave state is discussed.

1 Introduction

Using the Bethe-Salpeter (BS) equation [1] to describe the nucleon-nucleon (NN) interaction is one of the most consistent approaches. In this formalism, one has to deal with a system of nontrivial integral equations for the NN scattered states and for the bound state – the deuteron. To solve the system of integral equations it is convenient to use a separable ansatz [2] for the interaction kernel in the BS equation. In this case, one can transform integral equations into a system of algebraic linear ones which is easy to solve. Parameters of the interaction kernel are found from the analysis of phase shifts for respective partial-wave states and low-energy parameters as well as deuteron static properties (bound state energy, magnetic moment, etc.).

In our previous papers [3, 4] the multirank separable potentials for the description of the scattered neutron-proton (np) system with the total angular momentum $J = 0, 1$ and the bound state – the deuteron – were proposed. Various methods of a relativistic generalization of initially nonrelativistic separable functions parametrizing the interaction kernel were considered. The elaborated potentials allow us to describe the experimental data for the phase shifts up to the laboratory kinetic energy $T_{\text{Lab}} \sim 3$ GeV, static properties of the deuteron, and the exclusive electron-deuteron breakup in the plane-wave approximation [3–5].

However, it is well known that the influence of the inelastic channels concerned with non-nucleon degrees of freedom (mesons, Δ isobars, nucleon excitations, six-quark admixtures, etc.) becomes significant with increasing energy of the nucleon-nucleon system. To treat them in the elastic NN scattering the inelasticity parameter which is responsible for a proper flux behavior is introduced.

There are several methods to describe the inelasticity parameter (see e.g., [6, 7]). One of the way is to use a complex NN potential instead of the real-valued one. We apply this

idea to the relativistic separable interaction kernel obtained earlier [3,4]. At the same time we want to keep the results for observables below the inelasticity threshold and have a slight difference above it. To achieve this we consider the complex separable interaction kernel of a special type (Sec.3). A special procedure which we apply to find new imaginary interaction kernel parameters is described in Sec.4. The discussion and conclusion are given in Sec.5 and Sec.6, respectively.

2 Parametrization of the S matrix

In the paper, we use the Arndt-Roper parametrization [8] of the elastic NN scattering S matrix. For uncoupled partial-wave states, in the presence of inelasticity the S matrix is written via the K matrix as follows:

$$S = \frac{1 - K_i + iK_r}{1 + K_i - iK_r} = \eta \exp(2i\delta), \quad (1)$$

where real K_r and imaginary K_i parts of the K matrix ($K = K_r + iK_i$) are parametrized

$$K_r = \tan \delta, \quad K_i = \tan^2 \rho, \quad (2)$$

in terms the phase shift δ and the inelasticity parameter ρ , respectively, and

$$\begin{aligned} \eta^2 &= \frac{1 + K^2 - 2K_i}{1 + K^2 + 2K_i}, \\ K^2 &= K_r^2 + K_i^2. \end{aligned} \quad (3)$$

For elastic scattering ($\rho = 0$), $\delta = \delta_e$, $\eta = 1$ and $S = S_e = \exp(2i\delta_e)$.

3 Complex separable kernel

We assume that the interaction kernel V conserves parity, the total angular momentum J and its projection, and isotopic spin. Due to the tensor nuclear force, the orbital angular momentum L is not conserved. The negative-energy two-nucleon states are switched off, which leads to the total spin S conservation. The partial-wave-decomposed BS equation is, therefore, reduced to the following form:

$$\begin{aligned} T_{l'l}(p'_0, |\mathbf{p}'|; p_0, |\mathbf{p}|; s) &= V_{l'l}(p'_0, |\mathbf{p}'|; p_0, |\mathbf{p}|; s) \\ &+ \frac{i}{4\pi^3} \sum_{l''} \int_{-\infty}^{+\infty} dk_0 \int_0^{\infty} \mathbf{k}^2 d|\mathbf{k}| \frac{V_{l''l''}(p'_0, |\mathbf{p}'|; k_0, |\mathbf{k}|; s) T_{l''l}(k_0, |\mathbf{k}|; p_0, |\mathbf{p}|; s)}{(\sqrt{s}/2 - E_{\mathbf{k}} + i\epsilon)^2 - k_0^2}, \end{aligned} \quad (4)$$

where $l = l' = l''$ for spin-singlet and uncoupled spin-triplet states. The square of the np pair total momentum s is connected with the laboratory energy T_{Lab} as: $s = 2mT_{\text{Lab}} + 4m^2$, m is the mass of the nucleon.

To describe the inelasticity in the elastic NN scattering we modify the real-valued relativistic potential adding the imaginary part:

$$V_r \rightarrow V = V_r + iV_i.$$

To solve the Eq.(4) the separable (rank N) ansatz [2] for the NN interaction kernel is used:

$$V_{l'l}(p'_0, |\mathbf{p}'|; p_0, |\mathbf{p}|; s) = \sum_{m,n=1}^N [\lambda_{mn}^r(s) + i\lambda_{mn}^i(s)] g_i^{[l']}(p'_0, |\mathbf{p}'|) g_j^{[l]}(p_0, |\mathbf{p}|), \quad (5)$$

where the imaginary part λ^i has the form:

$$\lambda_{mn}^i(s) = \theta(s - s_{th}) \left(1 - \frac{s_{th}}{s}\right) \bar{\lambda}_{mn}^i, \quad (6)$$

$g_j^{[l]}$ are the model functions, $\lambda_{mn} = \lambda_{mn}^r + i\lambda_{mn}^i$ is a matrix of model parameters and s_{th} is the inelasticity threshold (the first energy point where the inelasticity becomes nonzero). In this case, the resulting T matrix has a similar separable form:

$$T_{l'l}(p'_0, |\mathbf{p}'|; p_0, |\mathbf{p}|; s) = \sum_{m,n=1}^N \tau_{mn}(s) g_i^{[l']}(p'_0, |\mathbf{p}'|) g_j^{[l]}(p_0, |\mathbf{p}|), \quad (7)$$

where

$$(\tau_{mn}(s))^{-1} = (\lambda_{mn}^r(s) + i\lambda_{mn}^i(s))^{-1} + h_{mn}(s), \quad (8)$$

$$h_{mn}(s) = -\frac{i}{4\pi^3} \sum_l \int dk_0 \int \mathbf{k}^2 d|\mathbf{k}| \frac{g_m^{[l]}(k_0, |\mathbf{k}|) g_n^{[l]}(k_0, |\mathbf{k}|)}{(\sqrt{s}/2 - E_{\mathbf{k}} + i\epsilon)^2 - k_0^2}. \quad (9)$$

It should be noted that functions $g_m^{[l]}$ and parameters λ^r coincide with those used in [3, 4] while λ^i are new parameters which are calculated.

The separable functions $g_m^{[l]}$ used in the representation (5) of the interaction kernel V are obtained by a relativistic generalization of initially nonrelativistic Yamaguchi-type functions depending on the 3-momentum squared $|\mathbf{p}|$. We introduce the imaginary part V_i of the potential V (5) adding the new parameters λ^i to the real part V_r which is left intact. Thus, we intend to describe the additional inelasticity parameters by a minimal change of the previous kernels [3, 4].

4 Calculations and results

We start from the real-valued interaction kernels which were obtained from the minimization of the squared derivative function χ^2 containing the phase shifts and the low-energy characteristics (details can be found in [3, 4]). Then we fix the parameters of the real part (λ^r , β and α) and calculate the parameters λ^i to describe the inelasticity.

The calculation is performed for all available experimental data for the phase shifts and the inelasticity parameters taken from the SAID program [9].

The minimization procedure for the function

$$\chi^2 = \sum_{m=m_{th}}^n (\delta^{\text{exp}}(s_m) - \delta(s_m))^2 / (\Delta\delta^{\text{exp}}(s_m))^2 + \sum_{m=m_{th}}^n (\rho^{\text{exp}}(s_m) - \rho(s_m))^2 / (\Delta\rho^{\text{exp}}(s_m))^2 \quad (10)$$

is used for every partial-wave state. Here n is a number of available experimental points. The number m_{th} corresponds to the data point with the first nonzero ρ value. It is defined by the threshold kinetic energy $T_{\text{Lab } th}$ which is taken from the single-energy analysis [9].

Table 1: Parameters $\bar{\lambda}^i$ of the rank-two kernel for P partial-wave states. (We would like to note misspells in Table 1 [3] where $\bar{\lambda}$ (GeV⁴) should be read as $\bar{\lambda}$ (GeV²) for the $^3P_0^+$ partial-wave state).

	MYI2		
	$^1P_1^+$	$^3P_0^+$	$^3P_1^+$
$\bar{\lambda}_{11}^i$ (GeV ⁴)	-0.007097474	97.12885	-0.007617132
$\bar{\lambda}_{12}^i$ (GeV ⁴)	-0.692547	-114.857	-0.3582908
$\bar{\lambda}_{22}^i$ (GeV ⁴)	-67.62616	-35.16663	-11.10021
$T_{Lab\ th}$ (GeV)	0.35	0.25	0.35

Table 2: Parameters $\bar{\lambda}^i$ of the rank-three kernel for the $^1S_0^+$ state. (We would like to note misspells in Table 2 [3] where $\bar{\lambda}$ (GeV²) should be read as $\bar{\lambda}$ (GeV⁰)).

MYI3	
$\bar{\lambda}_{11}^i$ (GeV ²)	-0.01332595
$\bar{\lambda}_{12}^i$ (GeV ²)	-89.63644
$\bar{\lambda}_{13}^i$ (GeV ²)	0.151908
$\bar{\lambda}_{22}^i$ (GeV ²)	-58097.6
$\bar{\lambda}_{23}^i$ (GeV ²)	2276.805
$\bar{\lambda}_{33}^i$ (GeV ²)	-217.6001
$T_{Lab\ th}$ (GeV)	0.3

Thus, given the real part of the separable potential the imaginary part parameters λ^i enable to describe the inelasticity with a minimal change of the phase shift description.

The obtained parameters λ^i are listed in Tables 1 and 2.

In Figs.1-4, the results of the phase shift and inelasticity parameter calculations (MYI2, MYI3 - red dashed line) are compared with the experimental data, our previous result without inelasticities [3,4] (MY2, MY3 - red solid line; only for phase shifts) and the SP07 solution [10] (green dashed-dotted line).

5 Discussion

In Fig.1, we see that all calculations (MY2, MYI2, SP07) give an excellent description of the phase shifts and two of them (MYI2, SP07) - of the inelasticity parameter for all available experimental data (up to $T_{Lab} \sim 1.1$ GeV) for the $^1P_1^+$ partial-wave state. However, their behavior is rather different at higher energies. To make a choice in favor of one of them experimental data in a wider energy range are necessary.

In Fig.2, the results of the calculations for the $^3P_0^+$ partial-wave state are shown. All of them (MY2, MYI2, SP07) demonstrate a reasonable agreement with the experimental data for the phase shifts in the whole energy range (up to $T_{Lab} \sim 3$ GeV).

The description of the inelasticity parameter is perfect for the MYI2 model and the SP07 solution up to $T_{Lab} \sim 3$ GeV (except the energy interval $T_{Lab} \sim 0.7 - 1.4$ GeV for MYI2). The

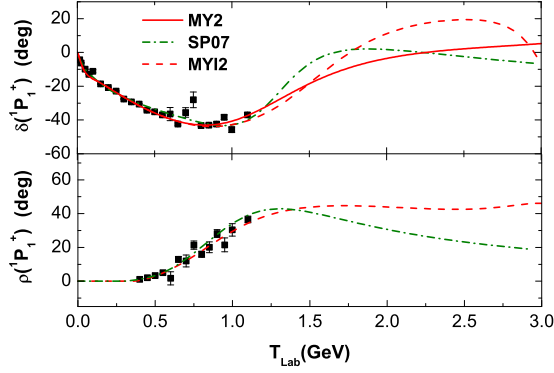


Figure 1: Phase shifts and inelasticity parameter for the $^1P_1^+$ partial-wave state.

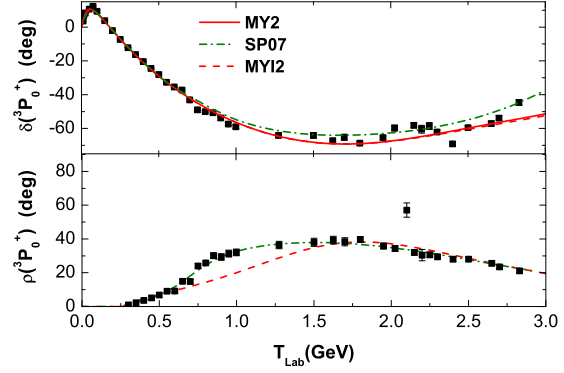


Figure 2: Phase shifts and inelasticity parameter for the $^3P_0^+$ partial-wave state.

behavior of the inelasticity parameter for the $^3P_0^+$ state in this energy range needs a separate discussion. Let us consider the difference

$$\Delta\eta(T_{\text{Lab}}) = (\eta^{\text{MYI2}}(T_{\text{Lab}}))^2 - (\eta^{\text{exp}}(T_{\text{Lab}}))^2, \quad (11)$$

Fig.5, which is analyzed using the Breit-Wigner formula

$$\Delta\eta(T_{\text{Lab}}) = C + \sum_{i=1,2} (2A_i/\pi) \frac{\Gamma_i}{4(T_{\text{Lab}} - M_i^*)^2 + \Gamma_i^2} \quad (12)$$

where A_i, C are constants, and M_i, Γ_i are the effective width and mass of the resonance systems, respectively. It is seen that the obtained distribution is in perfect agreement with $\Delta\eta$ in the considered energy range. It may be interpreted as a signal of two dybaryon resonances with masses $M_1^* = 2.27$ GeV, $M_2^* = 2.55$ GeV and widths $\Gamma_1 = 0.199$ GeV, $\Gamma_2 = 1.335$ GeV, respectively. Of course, this fact needs a more careful analysis in future.

The phase shifts and the inelasticity parameter for the $^3P_1^+$ partial-wave state are depicted in Fig.3. All results (MY2, MYI2, SP07) are acceptable in the limits of the experimental errors in the considered range of energies (up to $T_{\text{Lab}} \sim 3$ GeV). However, MYI2 and SP07 give rather different description for the inelasticity parameter. Nevertheless, an uncertainty in the experimental data values allows to accept both of them.

The $^1S_0^+$ partial-wave state is presented in Fig.4. It can be seen that all calculations show a perfect agreement with the measured phase shifts in the whole energy range (up to $T_{\text{Lab}} \sim 3$ GeV). The description of the inelasticity parameter by the MYI3 potential and the SP07 solution is also good.

It is seen that the proposed MYIN potentials give a consistent description of the existing experimental data for the phase shifts and the inelasticity parameter. It should be noted that since all parameters of the real separable interaction kernel (λ^r, β and α) found in the previous analysis [3,4] have been fixed, the phase shifts obtained using the MYN and MYIN models coincide up to $T_{\text{Lab}} < T_{\text{Lab}th}$ and are slightly different at $T_{\text{Lab}} > T_{\text{Lab}th}$ for all considered partial-wave states except $^1P_1^+$. The difference above $T_{\text{Lab}th}$ is explained by the influence of the imaginary part λ^i in the MYIN potential (see Eq.(6)).

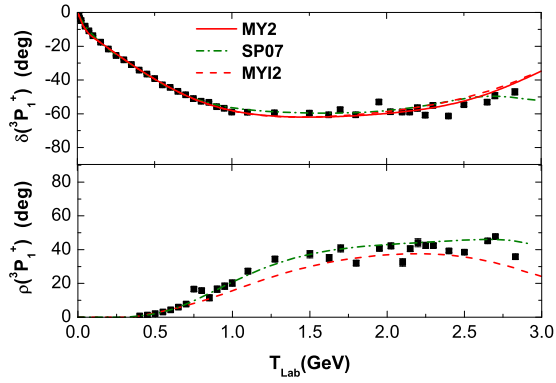


Figure 3: Phase shifts and inelasticity parameter for the $^3P_1^+$ partial-wave state.

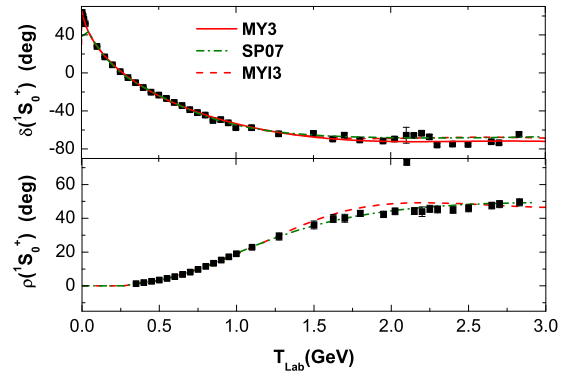


Figure 4: Phase shifts and inelasticity parameter for the $^1S_0^+$ partial-wave state.

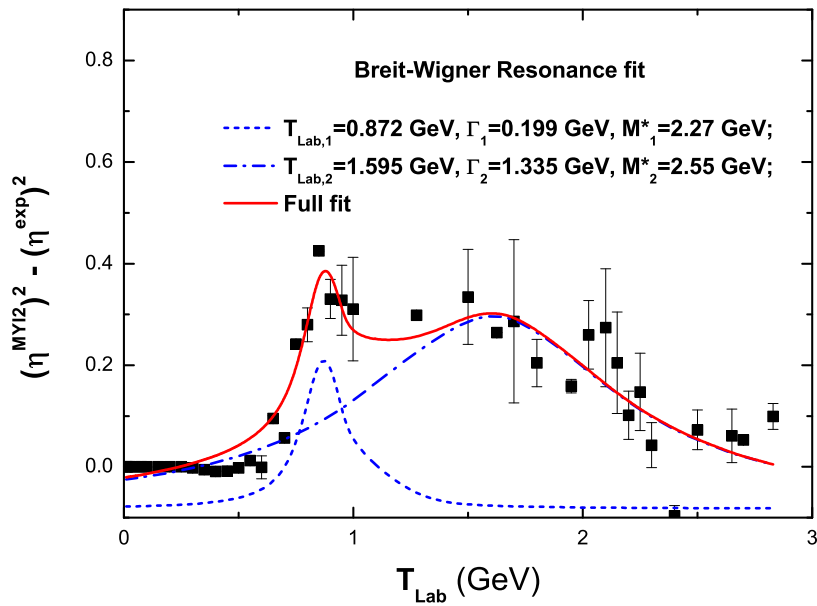


Figure 5: Difference $\Delta\eta$ for the $^3P_0^+$ partial-wave state.

6 Conclusion

The proposed complex potentials allow us to describe the inelasticity appearing in the elastic np scattering with increasing energy of the nucleons. They have been constructed by the introduction of the imaginary part (minimal extension) into the real-valued potentials elaborated earlier [3,4]. In this case, the low-energy characteristics and the phase shifts below the inelasticity threshold remain unchanged while above the threshold the obtained phase shifts slightly differ from the previous ones (except the $^1P_1^+$ partial-wave state).

The imaginary part parameters have been found from the description of the experimental data for the phase shifts and the inelasticity parameters for the laboratory energy up to 3 GeV.

The deviation of the MYI2 curve from the experimental values for the inelasticity parameter in the $^3P_0^+$ partial-wave state can be interpreted as a presence of the dybaryon resonances. However, this conclusion needs further investigation.

7 Acknowledgments

We are grateful to Professor V. Karmanov for stimulating questions and useful discussions.

References

- [1] E.E. Salpeter, H.A. Bethe, Phys. Rev. **84** (1951) 1232.
- [2] S.G. Bondarenko *et al.*, Prog. Part. Nucl. Phys. **48** (2002) 449, nucl-th/0203069.
- [3] S.G. Bondarenko *et al.*, Nucl. Phys. **A832** (2010) 233, 0810.4470 [nucl-th].
- [4] S.G. Bondarenko *et al.*, Nucl. Phys. **A848** (2010) 75, 1002.0487 [nucl-th].
- [5] S.G. Bondarenko, V.V. Burov, E.P. Rogochaya, Few Body Syst. **49** (2010) 121, 1008.0107 [nucl-th].
- [6] K.O. Eysler *et al.*, Eur. Phys. J. **A22** (2004) 105.
- [7] V.A. Knyr, V.G. Neudachin, N.A. Khokhlov, Phys. Atom. Nucl. **69** (2006) 2034; N.A. Khokhlov, V.A. Knyr, Phys. Rev. **C73** (2006) 024004.
- [8] R.A. Arndt, L.D. Roper, Phys. Rev. D **25** (1982) 2011; R.A. Arndt *et al.*, Phys. Rev. **D28** (1983) 97.
- [9] <http://gwdac.phys.gwu.edu>
- [10] R.A. Arndt *et al.*, Phys. Rev. **C76** (2007) 025209, 0706.2195 [nucl-th].